Enantioseparation and ecotoxicity evaluation of ibrutinib by Electrokinetic Chromatography using single and dual systems

Laura García-Cansino [a], Karina Boltes [a,b], María Luisa Marina [a,c], María Ángeles García [a,c,*]

[a] *Universidad de Alcalá, Departamento de Química Analítica, Química Física e Ingeniería Química, Ctra. Madrid-Barcelona Km. 33.600, 28871, Alcalá de Henares, Madrid, Spain*
[b] *IMDEA Water Institute, Parque Científico Tecnológico, E-28805, Alcalá de Henares, Madrid, Spain*
[c] *Universidad de Alcalá, Instituto de Investigación Química Andrés M. Del Río, Ctra. Madrid-Barcelona Km. 33.600, 28871, Alcalá de Henares, Madrid, Spain*

A B S T R A C T

In this work, two chiral methods enabling the separation of ibrutinib enantiomers were developed by Electrokinetic Chromatography. A cyclodextrin (CD) or a mixture of the CD and a chiral ionic liquid (CIL) was used as chiral selector. Using the single CD system, seven neutral and six anionic CDs were tested in a formate buffer at pH 3.0 working in positive and negative polarity, respectively. The use of sulfated-γ-CD (S-γ-CD) and negative polarity originated the best results considering analysis time and enantioresolution. The optimization of the experimental conditions allowed obtaining the separation of ibrutinib enantiomers in an analysis time of 4.2 min with an enantioresolution value of 1.5. The effect of the addition of fifteen CILs on the enantioresolution was evaluated showing that both analysis time and enantioresolution were generally increased. A mixture of S-γ-CD and [TMA][L-Lys] was selected which provided the separation of ibrutinib enantiomers in 8.1 min with an enantioresolution value of 3.3 under the same experimental conditions as in the case of using the single CD system. The enantiomeric impurity (S-ibrutinib) was the first-migrating isomer when using the single CD and the combined CD/CIL systems, as corresponds to the most desirable situation. Both chiral methods allowed the detection of the enantiomeric impurity up to a 0.1% as established by the International Council on Harmonization. After establishing the analytical characteristics of both chiral methodologies developed, they were applied to the enantiomeric determination of ibrutinib in a pharmaceutical formulation for hospital use marketed as pure enantiomer (R-ibrutinib) and to evaluate the stability and ecotoxicity of racemic ibrutinib and R-ibrutinib on *Daphnia magna*. The developed methodologies enabled, for the first time, the rapid chiral quantitation of ibrutinib in abiotic and biotic matrices.

1. Introduction

The population aging increases the use of pharmaceuticals, especially in the most developed countries. An important number of these drugs are chiral and, as the enantiomers of chiral drugs may have different properties, this fact has originated an increase in the number of drugs marketed as pure enantiomers [1]. Therefore, adequate analytical methodologies are necessary to carry out the quality control of these chiral drugs according to the International Council for Harmonization (ICH) guidelines, which establish that the enantiomeric impurity should not exceed a 0.1% with respect to the majority enantiomer [2,3]. In addition, in 2020, the EU legislation classified some pharmaceuticals (antibiotics and antidepressants) as priority contaminants of water, to

enhance their vigilance in aquatic environments [4]. But the chiral nature of many drugs and the enantioselective toxicity are not yet considered in risk evaluation of pharmaceuticals, even though the scientific community has spent several years reporting the importance of considering the stereochemistry of chiral drugs in the environment [5, 6]. Likewise, the use of antineoplastic agents for the treatment of cancer is continuously increasing and with it the appearance of these drugs in the aquatic environment. The potential danger of this family of drugs, many of them chiral, for the aquatic organisms is highly probable because they are non-specific drugs for tumor cells and therefore can cause toxicity in other non-target cells and organisms [7,8]. In general, anticancer drugs are recognized as the most toxic pharmaceuticals marketed around the world and have been classified as hazardous substances by the Waste Framework Directive of the European Commission

---

* Corresponding author. Universidad de Alcalá, Departamento de Química Analítica, Química Física e Ingeniería Química, Ctra. Madrid-Barcelona Km. 33.600, 28871, Alcalá de Henares, Madrid, Spain.
E-mail address: angeles.garcia@uah.es (M.Á. García).

Abbreviations

CILs	chiral ionic liquids
H_2DCFDA	$2',7'$-dichlorofluorescin diacetate
EC_{20}	effective concentration originating a 20% inhibition
EC_{50}	effective concentration originating a 50% inhibition
[EMIm][L-Lact]	1-ethyl-3-methylimidazolium l-lactate
DM-βCD	heptakis(2,6-di-O-methyl)-β-CD
[HETMAm][L-Lact]	2-hydroxyethyl-trimethylammonium l-lactate
HP-β-CD	2-hydroxypropyl-β-CD
HP-γ-CD	hydroxypropyl-γ-CD
ILs	ionic liquids
M-β-CD	methyl-β-CD
M-γ-CD	methyl-γ-CD
[L-Carn][NTf$_2$]	l-carnitine methyl ester bis(trifluoromethane) sulfonimide
[L-Carn][L-Lact]	l-carnitine methyl ester l-lactate
Ph-β-CD	phosphate-β-CD ()
Ph-γ-CD	phosphate-γ-CD

ROS	reactive oxygen species
RLOD	relative limit of detection
RRF	Response Relative Factor
S-β-CD	sulfated-β-CD
S-γ-CD	2-sulfated-γ-CD
SB-β-CD	sulfobutylated-β-CD
Captisol	sulfobutylether-β-CD
[TBA][L-Arg]	tetrabutylammonium-l-arginine
[TBA][L-Asp]	tetrabutylammonium-l-aspartic acid
[TBA][L-Glu]	tetrabutylammonium-l-glutamic acid
[TBA]$_2$[L-Glu]	2-tetrabutylammonium-l-glutamic acid
[TBA][L-Iso]	tetrabutylammonium-l-isoleucine
[TBA][L-Lys]	tetrabutylammonium-l-lysine
[TMA][L-Arg]	tetramethylammonium-l-arginine
[TMA][L-Asp]	tetramethylammonium-l-aspartic acid
[TMA][L-Glu]	tetramethylammonium-l-glutamic acid
[TMA][L-Iso]	tetramethylammonium-l-isoleucine
[TMA][L-Lys]	tetramethylammonium-l-lysine

[9]. In addition, several articles, focused on the environmental risk assessment of anticancer drugs, agree on the need to have more eco-toxicity data on these drugs. However, the aquatic ecotoxicity of this family of drugs has scarcely been studied and no stereoselective studies on this topic have been reported [10,11]. These reasons justify that the application of chiral analytical methodologies is of great interest in the study of the stability and ecotoxicity of these chiral contaminants, providing valuable information on the behavior of these compounds and their enantiomers in different non-target organisms.

Different separation techniques have shown a great potential to achieve chiral separations being High-Performance Liquid Chromatography (HPLC) and Capillary Electrophoresis (CE) the most used. The relevance of CE in the field of chiral analysis is related to different advantages [12], such as the fact that chiral columns are not necessary (although they can be used in the capillary electrochromatography (CEC) mode), the high efficiency and resolution than can be obtained, and the low consumption of reagents and samples which saves analysis costs [13] and make CE an environmentally friendly technique. In Electrokinetic Chromatography (EKC), which is the most used CE mode for chiral separations, the chiral selector is added to the separation buffer so it can easily be changed conferring to this technique a high flexibility for the separation of enantiomers based on this possibility. A great variety of chiral selectors is available such as cyclodextrins (CDs), macrocyclic antibiotics, bile salts, crown ethers, etc. Among them, CDs are the most employed chiral selectors in CE due to their high discrimination power, the wide variety of CD derivatives that exist, and their availability [13–17]. However, despite their great potential for chiral separations, the use of a CD as chiral selector does not assure a given enantiomeric separation. In these cases, the combination of two CDs or the addition of other compounds to the separation medium containing a CD have been proposed [16]. In this sense, the use of ionic liquids (ILs) [18,19] in CE has been considered an attractive alternative to other organic additives.

ILs are organic salts with a cationic counterpart which is organic and with an anionic counterpart which can be organic or inorganic [20]. CILs have melting points below 100 °C [21]. Normally, chiral ILs (CILs) are characterized by the fact that the cationic or the anionic part of the IL or both are chiral. According to the literature, tetraalkylammonium, amino acid, or azole groups are the most used in the synthesis of CILs as chiral cations while amino acids, lactic acid or camphorsulfonate are the most used as chiral anions [22]. These organic salts can be used in CE as additives to the separation system [23–29], as a single chiral selector [30–32] or as a ligand [33–35] although they can also adhere to the capillary inner wall as a coating [19]. Some works have reported that a synergistic effect can be originated when combining ILs with CDs although the improvement observed in the resolution between enantiomers was usually associated with an increase in the analysis time [17, 19,22,23,27,28].

Ibrutinib (1-[(3R)-3-[4-Amino-3-(4-phenoxyphenyl)-1H-pyrazolo [3,4-d]pyrimidin-1-yl]piperidin-1-yl]prop-2-en-1-one) (Fig. S1 in supplementary material) is a novel drug approved by the Food and Drug Administration (FDA) for the first time in 2013 [36]. It is a Bruton's tyrosine kinase (BTK) inhibitor with potential antineoplastic activity approved for multiple B-cell malignancies [37]. Ibrutinib contains a chiral center in its structure which gives rise to a pair of enantiomers, S-ibrutinib and R-ibrutinib (Fig. S1 in supplementary material). However, pharmaceutical formulations based on this drug are enantiomerically pure because only the R-enantiomer shows biological activity compared to S-enantiomer, which is the inactive enantiomer [38].

The separation of ibrutinib enantiomers has recently been reported by HPLC with UV detection using cellulose tris (3,5-dichlorophenylcarbamate) immobilized on silica gel (Chiral-pack-IC) using n-hexane:ethanol (55:45% v/v) with a 0.1% diethyl amine and 0.3% trifluoro acetic acid as mobile phase [37]. Under these conditions, the enantioseparation was obtained in around 21 min with a resolution above 4.0. However, no application was described for the analysis of a real sample. Our research group has modeled the enantiomeric separation of a multicomponent mixture of drugs by EKC, including ibrutinib, using mixtures of CDs as chiral selectors [39]. However, no work has described the rapid separation of ibrutinib enantiomers by EKC nor a method enabling the enantiomeric determination of ibrutinib in pharmaceutical formulations. Moreover, the stability and ecotoxicity of R, S-ibrutinib and R-ibrutinib as chiral emerging contaminants on non-target aquatic microorganisms have never been evaluated.

For these reasons, this work is aimed to develop and compare two chiral EKC methodologies based on the use of a single CD system or its combination with a CIL for the rapid separation of the enantiomers of ibrutinib, and their application, for the first time, to the enantiomeric analysis of ibrutinib-based pharmaceutical formulations marketed as enantiomerically pure (R-ibrutinib). In addition, both methods have also been applied to the assessment, for the first time, of the stability and ecotoxicity of R,S- ibrutinib and R-ibrutinib on the non-target aquatic microorganism *Daphnia magna* (*D. magna*).

2. Materials and methods

2.1. Reagents and samples

Water used was purified in a Millipore Milli-Q system (Bedford, MA, USA). Formic acid and sodium hydroxide (NaOH) were from Sigma-Aldrich (St. Louis, MO, USA). Dimethyl sulfoxide (DMSO) was from Merck (Darmstadt, Germany), and hydrochloric acid (HCl) and urea were from Scharlab S.L. (Barcelona, Spain).

Both neutral and anionic CDs were employed as chiral selectors in this work. The seven neutral CDs used were: γ-CD, 2-hydroxypropyl-γ-CD (HP-γ-CD, average degree of substitution (DS) 3.2), and methyl-γ-CD (M-γ-CD, DS 12) from Cyclolab (Budapest, Hungary), 2-hydroxypropyl-β-CD (HP-β-CD (DS 0.6), and β-CD from Fluka (Buchs, Switzerland), and methyl-β-CD (M-β-CD, DS 1.6–2.0), and heptakis (2,6-di-O-methyl)-β-CD (DM-β-CD) from Sigma-Aldrich. The six anionic CDs employed as chiral selectors were: sulfated-β-CD (S-β-CD, DS 12.0–15.0) from Sigma-Aldrich, sulfobutylated-β-CD (SB-β-CD, DS 6.3), sulfated-γ-CD (S-γ-CD, DS 10.0), phosphated-β-CD (Ph-β-CD, DS 4.0), and phosphated-γ-CD (Ph-γ-CD, DS 3.5) from Cyclolab, and sulfobutylether-β-CD (Captisol) from Cydex Pharmaceuticals (Lawrence, Kansas).

Tetrabutylammonium-l-aspartic acid ([TBA][L-Asp]), tetrabutylammonium-l-arginine ([TBA][L-Arg]), tetrabutylammonium-l-isoleucine ([TBA][L-Iso]), tetrabutylammonium-l-lysine ([TBA][L-Lys]), tetrabutylammonium-l-glutamic acid ([TBA][L-Glu]), 2-tetrabutylammonium-l-glutamic acid ([TBA]$_2$ [L-Glu]), tetramethylammonium-l-aspartic acid ([TMA][L-Asp]), tetramethylammonium-l-arginine ([TMA][L-Arg]), tetramethylammonium-l-isoleucine ([TMA][L-Iso]), tetramethylammonium-l-lysine ([TMA][L-Lys]), tetramethylammonium-l-glutamic acid ([TMA][L-Glu]), l-carnitine methyl ester l-lactate ([L-CarnMe][L-Lact]), and l-carnitine methyl ester bis(trifluoromethane) sulfonimide ([L-CarnMe][NTf$_2$]) were the CILs employed in this work based on l-amino acids and synthesized by the Center for Applied Chemistry and Biotechnology (CQAB) from the University of Alcalá. 2-Hydroxyethyl-trimethylammonium l-lactate ([HETMAm][L-Lact]) and 1-ethyl-3-methylimidazolium l-lactate ([EMIm][L-Lact]) were purchased from Sigma-Aldrich.

R-ibrutinib, and R,S-ibrutinib were from MedChem Express (Monmouth Junction, NJ, USA). The ibrutinib pharmaceutical formulation for hospital use was kindly donated by a hospital in Madrid (Spain).

Dormant eggs of *D. magna* and the concentrated saline solutions to prepare the freshwater standard medium for the organism cultivation, were purchased from MicroBioTests (Ghent, Belgium). The 2′,7′-dichlorofluorescin diacetate (H$_2$DCFDA) reactive was from Sigma Aldrich (Spain).

2.2. Apparatus

The CE instrument employed (model 7100) was from Agilent Technologies (Waldbronn, Germany) and was controlled with the HP 3DCE ChemStation software. Detection was carried out with a diode array detector (DAD) at 200 nm (bandwidth 4 nm). Uncoated fused-silica capillaries (50 μm I.D. × 58.5 cm total length (50 cm effective length)) from Polymicro Technologies (Phoenix, AZ, USA) were employed.

An OHAUS Adventurer Analytical Balance (Nänikon, Switzerland), a pHmeter (model 744) from Metrohm (Herisau, Switzerland), and an ultrasonic bath B200 from Branson Ultrasonic Corporation (Danbury, CO, USA) were employed.

Ecotoxicity test was carried out using an IBERCEX growth chamber (Spain). Images of the microinvertebrate were taken using a fluorescence microscopy LEICA DM IL LED FLUO from Leica Microsystems (Mannheim, Germany) using a FITC filter and LAS AX software.

2.3. CE conditions

The capillary was conditioned every day to ensure the repeatability between injections with 0.1 M sodium hydroxide for 2 min, Milli-Q water for 2 min, 0.1 M HCl for 2 min, Milli-Q water for 2 min again, and, finally, with BGE for 2 min. Each new capillary was conditioned with 1 M sodium hydroxide for 30 min, Milli-Q water for 15 min and buffer solution (25 mM sodium formate at pH 3.0) for 60 min. At the beginning of each working day, the capillary was flushed with 0.1 M sodium hydroxide for 10 min, Milli-Q water for 5 min, 0.1 M HCl for 2 min and BGE for 10 min. Optimized conditions for the separation were: 25 mM formate buffer at pH 3.0, a separation voltage of −30 kV (negative-polarity) at a temperature of 30 °C, and injecting the solutions and samples at a pressure of 50 mbar for 5 s.

2.4. Preparation of solutions and samples

2.4.1. Preparation of solutions

To prepare the buffer solution, the adequate volume of formic acid was dissolved in Milli-Q water, the pH was adjusted to 3.0 with 1 M sodium hydroxide, and the final volume was completed with Milli-Q water. The necessary amounts of CDs or CDs and CILs were dissolved in the formate buffer solution to prepare the BGE at the desired concentrations.

2.4.2. Synthesis of CILs

Except for the two commercial ILs ([HETMAm][L-Lact] and [EMIm] [L-Lact]), the others ([TBA][L-Asp], [TBA][L-Arg], [TBA][L-Iso], [TBA] [L-Lys], [TBA][L-Glu], [TBA]$_2$[L-Glu], [TMA][L-Asp], [TMA][L-Arg], [TMA][L-Iso], [TMA][L-Lys], [TMA][L-Glu], [L-CarnMe][L-Lact] and [L-CarnMe][NTf$_2$]) were synthesized by the Center for Applied Chemistry and Biotechnology (CQAB) from the University of Alcalá following the procedures previously described in the literature [21,26,40].

2.4.3. Preparation of standard solutions of ibrutinib and pharmaceutical formulation solutions

R-ibrutinib and R,S-ibrutinib stock standard solutions were prepared at a concentration of 600 mg L^{-1} each in DMSO. Standard working solutions at different concentrations were obtained by dilution of these solutions in the BGE (composed of the CD in 25 mM formate buffer at pH 3.0).

To prepare a solution of the pharmaceutical formulation for hospital use, the appropriate amount of ibrutinib powder was weighed and dissolved in DMSO to obtain a concentration of 210 mg L^{-1} of R-ibrutinib according to the label. This solution was filtered to remove any remaining undissolved impurities to avoid interferences. From this solution, sample working solutions were prepared by dilution in the BGE (composed of the CD in 25 mM formate buffer at pH 3.0).

Before use, the filtration of all solutions was achieved through disposable nylon 0.45 μm pore size filters from Scharlau (Barcelona, Spain).

Both standard solutions and samples were stored at 4 °C.

2.5. Toxicity tests and stability evaluation

The stability of R-ibrutinib and R,S-ibrutinib was assessed under abiotic and biotic conditions using the same culture medium and incubation temperature as in ecotoxicity runs. Initial concentrations of R-ibrutinib and R,S-ibrutinib ranging from 2 to 30 mg L^{-1} and from 4 to 60 mg L^{-1}, respectively, were incubated in parallel without light, in presence and absence of *D. magna* specimens (biotic assays). Four replicates were carried out for each concentration, similarly to the biotic incubation in ecotoxicity tests. Samples were taken at 0, 24 and 48 h of incubation at 20 ± 2 °C. Concentration of enantiomers were determined by duplicate at initial and final incubation times.

Toxicity tests with *D. magna* were carried out following the

standardized procedure OECD Test Guideline 202 [41]. First, the dormant eggs of the microcrustacean were incubated in standard medium during 72 h at a temperature of 20 ± 2 °C, under continuous illumination of 6000 lux for the hatching.

Stock solutions of 2000 mg L^{-1} were prepared for R-ibrutinib and R, S-ibrutinib in DMSO. From these solutions, diluted solutions were prepared in the culture medium at ten different concentrations (from 2 to 30 mg L^{-1} for R-ibrutinib and from 4 to 60 mg L^{-1} for R,S-ibrutinib) and employed in the ecotoxicity assays. A non-toxic control assay (0 mg L^{-1}) was also employed. Each test condition was replicated four times.

Five young and actively swimming organisms per well were exposed to the contaminants in darkness conditions, during 48 h at the same temperature used during eggs hatching. Negative effects caused by R-ibrutinib and R,S-ibrutinib were daily evaluated by visual counting of swimming specimens. The EC$_{50}$ and EC$_{20}$ values are the parameters used to express the acute toxicity in terms of the loss of swimming capability of the specimens. These values are the real concentrations of ibrutinib racemate and R-ibrutinib causing the immobilization of 50% or 20% of organisms, respectively, during the exposure time. Ecotoxicity parameters were determined for 24 and 48 h of exposition time, using the control experiment (without pharmaceuticals) as the reference test with 0% inhibition. For the calculation of these parameters, experimental data of mobility inhibition vs drug concentration were adjusted to the median-effect/combination index (CI)-isobologram equation using CompuSyn software [42].

The generation of ROS was determined in specimens collected at 24 h of cultivation under the same conditions used for the ecotoxicity test, like in previous works [43,44]. Three organisms were captured from the culture medium without pharmaceuticals, exposed to 10 mg L^{-1} of R-ibrutinib and 20 mg L^{-1} of R,S-ibrutinib, and then incubated. These concentrations were selected in accordance with the EC$_{50}$ values obtained in the ecotoxicological study. The collected intact animals (without homogenization) were incubated during 2 h at 20 °C in 1 mL of 10 mM H$_2$DCFDA solution. Fluorescence generated was observed by microscopy (465–495 nm/515–555 nm ranges of excitation/emission wavelengths).

2.6. Data treatment

Chemstation software from Agilent Technologies provided migration times, peak areas, and resolution values (Rs). Corrected peak areas (Ac) (peak area divided by the corresponding retention time of each enantiomer) were employed to improve data reproducibility. Excel Microsoft, Origin Pro8 and Statgraphics Centurion XVII software were used for the experimental data analysis, calculate all required parameters and statistical tests, and the composition of graphs. CompuSyn software was used for the calculation of dose-effect parameters.

3. Results and discussion

3.1. Enantioseparation of ibrutinib by EKC using a single CD system

Considering the pKa value of ibrutinib (3.74 [45]), a 100 mM formate buffer at pH 3.0 was employed for preliminary experiments in order to have this compound positively charged. Two screenings were carried out both in positive polarity (+20 kV) with seven neutral CDs (β-CD, γ-CD, HP-β-CD, HP-γ-CD, M-β-CD, M-γ-CD, DM-β-CD) and in negative polarity (−20 kV) with six anionic CDs (S-β-CD, SB-β-CD, S-γ-CD, Ph-β-CD, Ph-γ-CD, Captisol). A 10 mM CD concentration and a temperature of 20 °C were employed in these assays. Results revealed that the discrimination between ibrutinib enantiomers was possible in positive polarity with M-γ-CD and in negative polarity with S-γ-CD. In the first case, the analysis time was 28.0 min and the enantioresolution was 1.6 (see Fig. S2). However, when using S-γ-CD as chiral selector, the separation took place in an analysis time of 9.0 min with a resolution of 2.0 (Fig. S2). Therefore, S-γ-CD was selected as the chiral selector for the

separation of ibrutinib enantiomers in negative polarity. Although a 50 mbar × 10 s injection was employed in these experiments, 50 mbar × 5s was used for injection in the following experiments since it was shown that, under these conditions, better peak shape and increased resolution were obtained.

The influence of the buffer concentration, CD concentration, and temperature was investigated. Concentration of formate buffer at pH 3.0 was varied from 25 to 150 mM (25, 50, 100, 150 mM). In order to short analysis time as much as possible, a 25 mM buffer concentration was chosen since the baseline separation of enantiomers was obtained under these conditions in 7.7 min as shown in Fig. 1A and Table S1 in supplementary material. Fig. 1 also shows that the enantiomeric impurity (S-ibrutinib) was the first-migrating enantiomer as it is desirable to facilitate the determination of this isomer in the presence of the majority one (the active R-ibrutinib enantiomer). Different values of the S-γ-CD concentration were tested (0.5, 1.0, 2.0, 3.0, 5.0, and 10.0 mM) and a concentration of 2 mM was selected to save method costs (due to the CD), by keeping the baseline separation of ibrutinib without increasing analysis time (see Fig. 1B and Table S1 in supplementary material). The effect of the temperature was studied by testing 20, 25, and 30 °C. As shown in Fig. 1C, a value of 30 °C gave rise to a resolution of 1.7 in a shorter analysis time (6.4 min) so this value was chosen as the most adequate. Under these optimized conditions, the effect of the addition of CILs on the separation of ibrutinib enantiomers was investigated.

3.2. Effect of chiral ionic liquids on the enantioseparation of ibrutinib

Fifteen CILs were added to the separation buffer under the optimal experimental conditions so far (25 mM formate buffer at pH 3.0, at 30 °C and applying a voltage of −20 kV) using 2 mM S-γ-CD as chiral selector to study a possible synergistic effect originating an improvement in the enantioresolution value and selectivity. Table S2 groups the different CILs studied in this work together with the analysis time, resolution values, peak areas and heights, and electrical currents obtained when each CIL was added at two concentration values (5 and 10 mM) to the separation buffer containing the CD. CILs based on L-Asp, L-Arg, L-Iso, L-Lys, or L-Glu as anionic counterion had a tetraalkylammonium salt as cationic counterpart (TBA or TMA). In the case of L-Glu, [TBA]$_2$[L-Glu] was also tested. CILs with L-Lact as anionic counterion had as cationic part L-CarnMe, HETMAm or EMIm. A final CIL based on L-CarnMe as cationic part had L-NTf$_2$ as anionic counterpart. Table S2 shows that the addition of a CIL can have a significant favorable effect on the enantioresolution value of ibrutinib, although an increase in the migration times was also observed. Results revealed that in the case of amino acids-based CILs, those composed of TMA gave generally better results than those composed of TBA and that a 5 mM concentration of CIL enabled to observe interesting increases in resolution with a minor cost referred to the amount of CIL employed. In fact, a 10 mM concentration of these CILs had no significant effects compared with the 5 mM concentration although slightly longer analysis times were obtained. Moreover, in some cases, such as for the CILs composed of [L-Arg] and [L-Lys], peaks disappeared, and baseline was deformed when the concentration of CIL was 10 mM. This result could be due to the increase in the ionic strength related to higher concentrations of CILs that would generate a high Joule heat, decreasing the separation efficiency. The highest values for the enantiomeric resolution at a 5 mM concentration of the CIL in the mixture with the CD were observed for [TMA][L-Arg] and [TMA][L-Lys]. Due to the better peak shapes obtained for [TMA][L-Lys], this CIL was selected to be combined with the CD to achieve the separation of ibrutinib enantiomers using the dual system. As indicated in previous works, the effects related to the addition of CILs in dual systems with CDs can be associated to a change in the characteristics of the separation buffer (viscosity, conductivity, ionic strength), and also to the existence of interactions between the ions of the CIL and the CD that can in turn alter the existing interactions between the enantiomers and the CD itself [17,19,22–24,27,28].
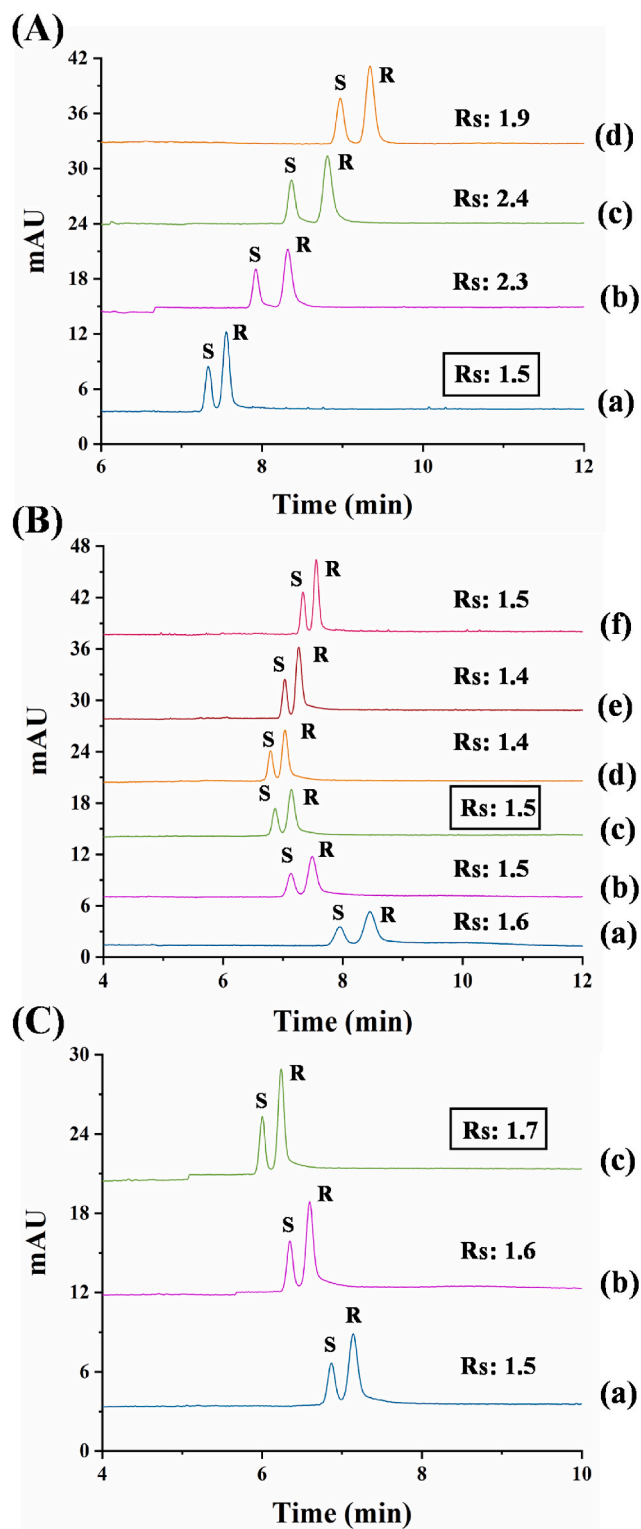
Fig. 1. Electropherograms corresponding to the enantioseparation of ibrutinib in a standard solution containing 15 and 30 mg L^{-1} of S- and R-ibrutinib, respectively: **(A)** 10 mM S-γ-CD in **(a)** 25 mM, **(b)** 50 mM, **(c)** 100 mM, and **(d)** 150 mM formate buffer at pH 3.0 at a temperature of 20 °C; **(B)** S-γ-CD at different concentrations: **(a)** 0.5 mM, **(b)** 1 mM, **(c)** 2 mM, **(d)** 3 mM, **(e)** 5 mM, and **(f)** 10 mM in 25 mM formate buffer at pH 3.0 at a temperature of 20 °C; **(C)** 2 mM S-γ-CD in 25 mM formate buffer at pH 3.0 at a temperature of: **(a)** 20 °C, **(b)** 25 °C, and **(c)** 30 °C. Experimental conditions: voltage: −20 kV; uncoated fused-silica capillary, 58.5 cm (50 cm effective length) x 50 μm i. d.; hydrodynamic injection: 50 mbar × 5 s; λ: 200 nm ± 4 nm.

In order to achieve a reduction in the analysis times without significantly decreasing the resolution values, different separation voltages were tested (−20 kV, −25 kV, −30 kV) for the single CD system as well as for the dual CD/CIL system. As shown in Fig. 2 and Table S1 in supplementary material, for both systems, −30 kV enabled to reduce the analysis time to 4.2 and 8.1 min, with enantioresolutions of 1.5 and 3.3, respectively.

The performance of both developed methods for the enantiomeric determination of ibrutinib in a pharmaceutical formulation were compared (single S-γ-CD system: 25 mM formate buffer at pH 3.0 with 2 mM S-γ-CD, 30 °C and −30 kV; dual S-γ-CD/[TMA][L-Lys] system: 25 mM formate buffer at pH 3.0 with 2 mM S-γ-CD + 5 mM [TMA][L-Lys], 30 °C and −30 kV).
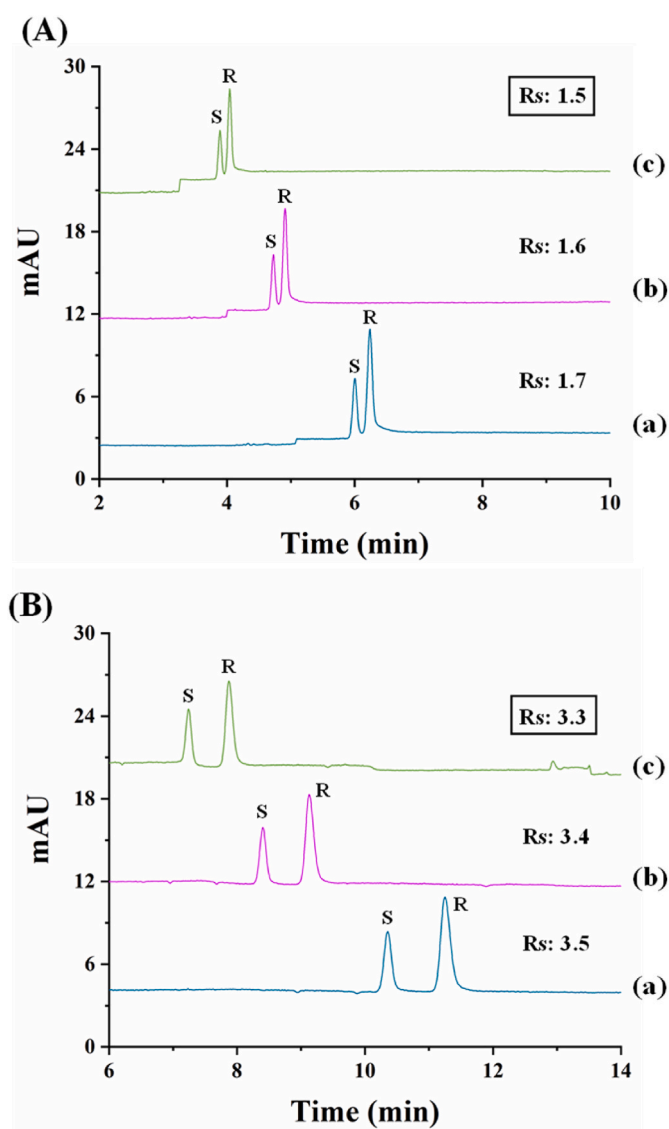
Fig. 2. Electropherograms corresponding to the enantioseparation of ibrutinib in a standard solution containing 15 and 30 mg L^{-1} of S- and R-ibrutinib, respectively, using: **(A)** a single system (2 mM S-γ-CD), or **(B)** a dual system (2 mM S-γ-CD + 5 mM [TMA][L-Lys]) with a 25 mM formate buffer at pH 3.0 at different separation voltages: **(a)** −20 kV, **(b)** −25 kV, and **(c)** −30 kV, at a temperature of 30 °C. Other experimental conditions as in Fig. 1.

3.3. Enantiomeric determination of ibrutinib in a pharmaceutical formulation

To apply the two chiral methodologies developed to the enantiomeric determination of ibrutinib in a pharmaceutical formulation, the analytical characteristics of both methods were evaluated in terms of selectivity, linearity, accuracy, precision, limits of detection (LOD) and limits of quantitation (LOQ). Tables 1 and 2 group the results obtained when the single S-γ-CD and the dual S-γ-CD/[TMA][L-Lys] systems were employed.

Fig. 3 shows the electropherograms obtained for the analysis of the pharmaceutical formulation by the two developed methodologies showing an adequate selectivity in both cases since no interferences

Table 1

Analytical characteristics of the EKC methodology developed for the determination of ibrutinib enantiomers using 2 mM S-γ-CD as chiral selector. Separation voltage −30 kV. Other experimental conditions as in Fig. 2.

	S-Ibrutinib	R-Ibrutinib
External standard calibration method[a]		
Range	0.5–10 mg L^{-1}	0.5–40 mg L^{-1}
Slope $\pm$ t x S$_{slope}$	0.24 $\pm$ 0.02	0.229 $\pm$ 0.004
Intercept $\pm$ t x S$_{intercept}$	−0.05 $\pm$ 0.09	−0.03 $\pm$ 0.08
R^2	99.4%	99.9%
p-value of ANOVA[b]	0.2743	0.0836
Standard additions calibration method[c]		
Pharmaceutical formulation		
Range	0–10 mg L^{-1}	0–20 mg L^{-1}
Slope $\pm$ t x S$_{slope}$	0.23 $\pm$ 0.06	0.23 $\pm$ 0.01
R^2	99.8%	99.4%
p-value of *t*-test[d]	0.1596	0.1438
Accuracy[e]		
Recovery (%)	99 $\pm$ 3	98 $\pm$ 4
Precision	5 mg L^{-1}	30 mg L^{-1}
Instrumental repeatability[f]		
t, RSD (%)	0.5	0.7
A$_c$, RSD (%)	3.2	1.1
Method repeatability[g]		
t, RSD (%)	2.0	1.3
A$_c$, RSD (%)	3.7	3.5
Intermediate precision[h]		
t, RSD (%)	1.5	1.6
Ac, RSD (%)	2.9	3.0
LOD[i]	0.1 mg L^{-1}	0.1 mg L^{-1}
LOQ[i]	0.5 mg L^{-1}	0.5 mg L^{-1}

A$_c$: corrected peak area.

[a] Five (for the S-enantiomer) and nine (for the R-enantiomer) ibrutinib standard racemate solutions at different concentration levels injected in triplicate.

[b] p-value for ANOVA to confirm that experimental data fit properly to linear models.

[c] Addition of five known amounts of ibrutinib standard racemate solution to a pharmaceutical formulation solution containing a constant concentration of R-ibrutinib (20 mg L^{-1}) according to the label.

[d] p-values of *t*-test should be > 0.05 at a confidence level of 95% which demonstrates absence of matrix interferences.

[e] Evaluated as the mean recovery obtained for ibrutinib enantiomers when six individual solutions of the pharmaceutical formulation (n = 6) containing 20 mg L^{-1} of R-ibrutinib (according to the label) were spiked with 10 mg L^{-1} and 20 mg L^{-1} of ibrutinib standard racemate.

[f] Six repeated injections (n = 6) of an ibrutinib standard racemate solution at a concentration of 10 mg L^{-1} in the case of the S-enantiomer and of the pharmaceutical formulation solution at 30 mg L^{-1} (according to the label) for the R-enantiomer.

[g] Three replicates injected three times each (n = 9) on the same day of an ibrutinib standard racemate solution at a concentration of 10 mg L^{-1} in the case of the S-enantiomer and of the pharmaceutical formulation solution at 30 mg L^{-1} (according to the label) for the R-enantiomer.

[h] Three replicates injected in triplicate (n = 9) during three consecutive days of an ibrutinib standard racemate solution at a concentration of 10 mg L^{-1} in the case of the S-enantiomer and of the pharmaceutical formulation solution at 30 mg L^{-1} (according to the label) for the R-enantiomer.

[i] Calculated experimentally.

Table 2

Analytical characteristics of the EKC methodology developed for the determination of ibrutinib enantiomers using the 2 mM S-γ-CD + 5 mM [TMA][L-Lys] dual system. Separation voltage −30 kV. Other experimental conditions as in Fig. 2.

	S-Ibrutinib	R-Ibrutinib
External standard calibration method[a]		
Range	0.5–10 mg L^{-1}	0.5–40 mg L^{-1}
Slope $\pm$ t x S$_{slope}$	0.23 $\pm$ 0.02	0.213 $\pm$ 0.008
Intercept $\pm$ t x S$_{intercept}$	1.1 $\pm$ 0.1	0.1 $\pm$ 0.1
R^2	99.6%	99.6%
p-value of ANOVA[b]	0.1761	0.1512
Standard additions calibration method[c]		
Pharmaceutical formulation		
Range	0–10 mg L^{-1}	0–20 mg L^{-1}
Slope $\pm$ t x S$_{slope}$	0.22 $\pm$ 0.02	0.212 $\pm$ 0.005
R^2	99.1%	99.8%
p-value of *t*-test[d]	0.1900	0.8494
Accuracy[e]		
Recovery (%)	102 $\pm$ 4	100 $\pm$ 3
Precision	5 mg L^{-1}	30 mg L^{-1}
Instrumental repeatability[f]		
t, RSD (%)	1.7	0.7
A$_c$, RSD (%)	2.0	1.5
Method repeatability[g]		
t, RSD (%)	2.1	1.7
A$_c$, RSD (%)	1.7	5.5
Intermediate precision[h]		
t, RSD (%)	3.3	4.0
Ac, RSD (%)	2.0	5.4
LOD[i]	0.1 mg L^{-1}	0.1 mg L^{-1}
LOQ[i]	0.5 mg L^{-1}	0.5 mg L^{-1}

A$_c$: corrected peak area.

[a] Five (for the S-enantiomer) and eight (for the R-enantiomer) ibrutinib standard racemate solutions at different concentration levels injected in triplicate.

[b] p-value for ANOVA to confirm that experimental data fit properly to linear models.

[c] Addition of six known amounts of ibrutinib standard racemate solution to a pharmaceutical formulation sample containing a constant concentration of R-ibrutinib (20 mg L^{-1}) according to the label.

[d] p-values of *t*-test (ANOVA) should be > 0.05 at a confidence level of 95% which demonstrated absence of matrix interferences.

[e] Evaluated as the mean recovery obtained for ibrutinib enantiomers when six individual solutions of the pharmaceutical formulation (n = 6) containing 20 mg L^{-1} of R-ibrutinib (according to the label) were spiked with 10 mg L^{-1} and 20 mg L^{-1} of ibrutinib standard racemate.

[f] Six repeated injections (n = 6) of an ibrutinib standard racemate solution at a concentration of 10 mg L^{-1} in the case of the S-enantiomer and of the pharmaceutical formulation solution at 30 mg L^{-1} (according to the label) for the R-enantiomer.

[g] Three replicates injected three times each (n = 9) on the same day of an ibrutinib standard racemate solution at a concentration of 10 mg L^{-1} in the case of the S-enantiomer and of the pharmaceutical formulation solution at 30 mg L^{-1} (according to the label) for the R-enantiomer.

[h] Three replicates injected in triplicate (n = 9) during three consecutive days of an ibrutinib standard racemate solution at a concentration of 10 mg L^{-1} in the case of the S-enantiomer and of the pharmaceutical formulation solution at 30 mg L^{-1} (according to the label) for the R-enantiomer.

[i] Calculated experimentally.

were observed.

To evaluate linearity, different standard solutions of ibrutinib racemate at different concentration levels from 1.0 mg L^{-1} to 80 mg L^{-1} were analyzed. For each enantiomer, calibration curves were obtained at different concentrations (for S-ibrutinib, from 0.5 to 10 mg L^{-1}, and for R-ibrutinib, from 0.5 to 40 mg L^{-1}) in both cases by plotting corrected peak areas (Ac) versus the concentration of each enantiomer in mg L^{-1} (see Tables 1 and 2). R^2 values were higher than 99.1%. Also, the confidence interval for the slopes did not include the zero value whereas that of the intercept included the zero value (for a 95% confidence level in both cases). Furthermore, it was confirmed that the experimental data
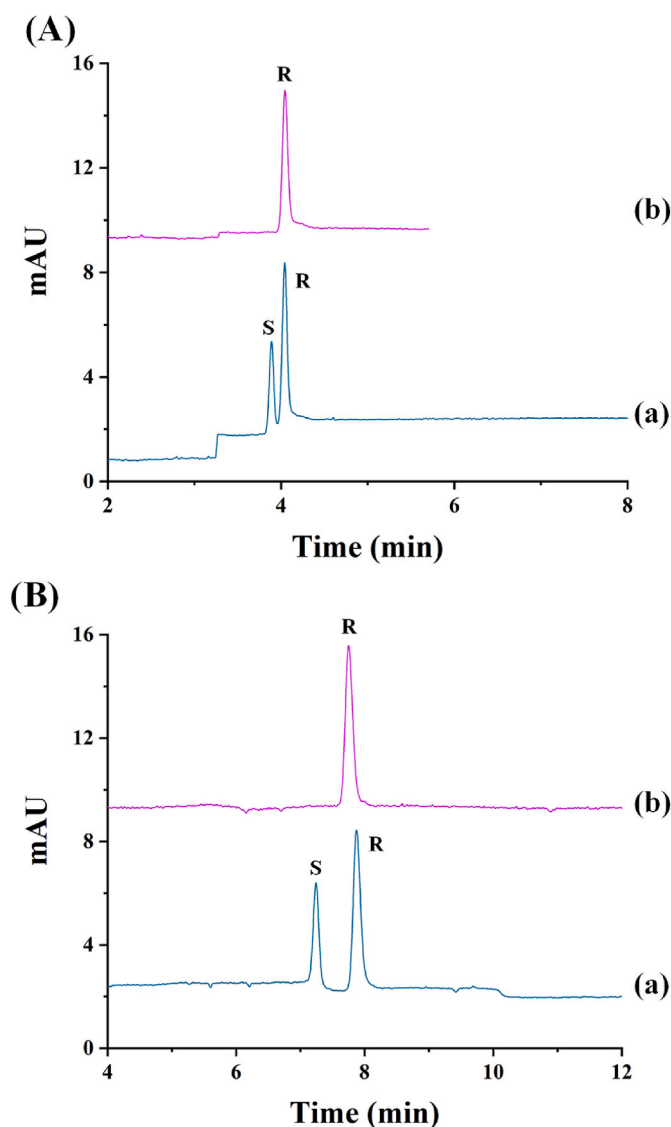
(A)

(B)

Fig. 3. Electropherograms corresponding to the enantioseparation of ibrutinib using: **(A)** a single system (2 mM S-γ-CD), and **(B)** a dual system (2 mM S-γ-CD + [TMA][L-Lys]). **(a)** Standard solution containing 15 mg L^{-1} and 30 mg L^{-1} of S- and R-ibrutinib, respectively; and **(b)** pharmaceutical formulation for hospital use containing 30 mg L^{-1} of R-ibrutinib. Separation voltage −30 kV. Other experimental conditions as in Fig. 2.

fitted correctly to a linear model by performing an ANOVA test (p-values obtained were > 0.05 for both systems). The Response Relative Factor (RRF, calculated by dividing the slope value of the majority enantiomer by the slope value of the minority enantiomer) was 0.9 for the single system and 1.0 for the dual system, which showed that the responses of both enantiomers were equivalent according to the European Pharmacopeia [46] that establishes that RRF should be comprised between 0.8 and 1.2. If the enantiomers responses are equivalent, their concentration ratio can be expressed as the ratio between their corrected peak areas.

The existence of matrix interferences for both developed methods was investigated. With this aim, the slopes corresponding to the external standard and the standard additions calibration methods were compared when different amounts of ibrutinib racemate were added to the pharmaceutical formulation, which contained a constant concentration of R-ibrutinib (see Tables 1 and 2). For both methods, there were not statistically significant differences between the slopes (p-values >0.05 for a confidence interval of 95%) so it could be concluded that there were no matrix interferences, and that the external standard calibration method

could be used for the enantiomeric determination of ibrutinib in the pharmaceutical formulation.

Accuracy was determined as the mean recovery (in percentage) for ibrutinib enantiomers by both developed methods when solutions of the pharmaceutical formulation containing 20 mg L^{-1} R-ibrutinib according to the label were spiked with ibrutinib standard racemate standard solution. As can be seen in Table 1, recovery values for the pharmaceutical formulation of 99 ± 3 and 98 ± 4 were obtained for S-ibrutinib and R-ibrutinib, respectively, when the single CD system was employed. For the dual CD/CIL system, recovery values obtained were 102 ± 4 and 100 ± 3 for S-ibrutinib and R-ibrutinib, respectively (see Table 2). In all cases, the recovery values were acceptable as they include the 100% value.

Precision of each method was determined for both enantiomers as instrumental repeatability, method repeatability and intermediate precision for corrected peak areas and migration times. An ibrutinib standard racemate solution at a concentration of 10 mg L^{-1} was used to evaluate the precision in the case of the S-enantiomer and a solution of the pharmaceutical formulation at a concentration 30 mg L^{-1} (according to the label) was used to evaluate the precision for the R-enantiomer. RSD values (%) for both migration times and corrected peak areas are included in Tables 1 and 2 for both methods. RSD values were below 2.0% and 3.7% for migration times and corrected peak areas, respectively, in the case of the single CD system, while for the dual system they were lower than 4.0 and 5.5%, respectively.

LOD and LOQ values were experimentally determined, being 0.1 mg L^{-1} and 0.5 mg L^{-1}, respectively, for both methods and both enantiomers. The relative limit of detection (RLOD) was calculated from the LOD experimentally obtained ((LOD for the minor enantiomer/concentration of the major enantiomer injected) x 100) using a nominal value of 100.0 mg L^{-1} of R-ibrutinib. The RLOD was 0.1% for both methods, which agrees with the legal ICH requirements [3]. Therefore, both chiral methods can detect up to a 0.1% of the enantiomeric impurity with respect to the majority enantiomer, although the use of the dual system enables to keep a higher enantiomeric resolution even at very high concentrations of the active enantiomer at the expense of the analysis time, under the same experimental conditions as those used with the single CD system. Fig. 4A and C shows the analysis of a solution of the pharmaceutical formulation at a concentration of 100 mg L^{-1} while the electropherograms corresponding to the analysis of a standard solution of R-ibrutinib (100 mg L^{-1}) spiked with S-ibrutinib at a concentration of 0.1 mg L^{-1} (0.1% enantiomeric impurity) are shown in Fig. 4B and D.

For the analysis of the pharmaceutical formulation, a sample solution containing 20 mg L^{-1} of R-ibrutinib according to the label was injected six times using each of the developed methodologies. Contents determined by both methods were 143 ± 3 mg per capsule, corresponding to a percentage of 102 ± 2% of the labeled content (140 mg per capsule) in both cases. The enantiomeric impurity (S-ibrutinib) was not detected in the pharmaceutical formulation in any case.

Results obtained show the potential of both EKC developed methodologies for the enantiomeric determination of ibrutinib in pharmaceutical formulations enabling their appropriate quality control.

3.4. Ecotoxicity evaluation of R,S-ibrutinib and R-ibrutinib on Daphnia magna

The analytical characteristics of both methods were also evaluated for the enantiomeric determination of ibrutinib enantiomers on *D. magna* culture medium in the same way as in the previous section. Table 3 groups the results obtained in the evaluation of the existence of matrix interferences, accuracy, precision, LOD and LOQ when the single S-γ-CD and the dual S-γ-CD/[TMA][L-Lys] systems were employed.

In order to investigate the existence of matrix interferences for both developed methods, the slopes corresponding to the external standard (Tables 1 and 2) and the standard additions calibration methods
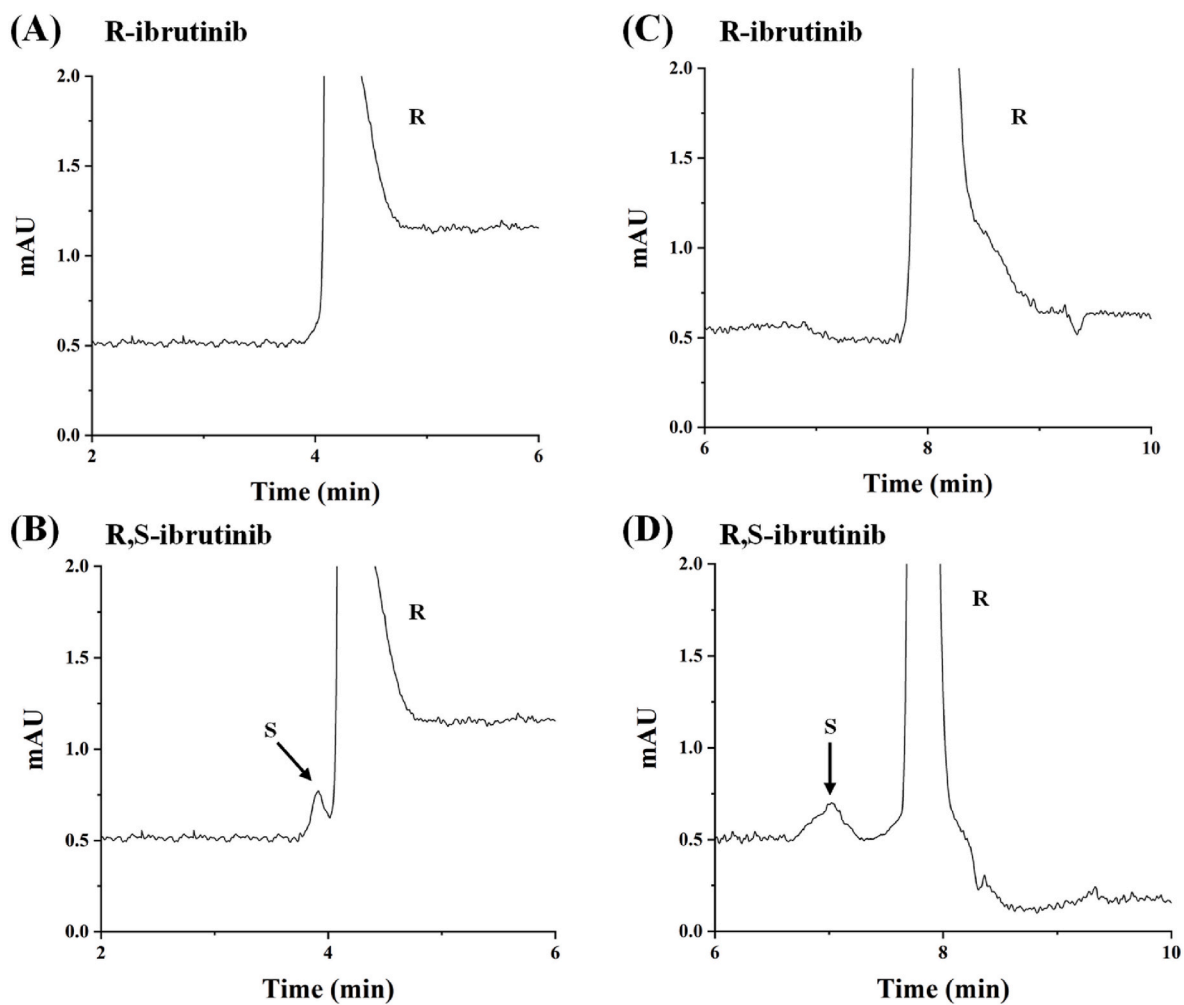
Fig. 4. Electropherograms corresponding to the analysis of a solution of the pharmaceutical formulation 100 mg L^{-1} in R-ibrutinib (**A** and **C**) and of a standard solution of R-ibrutinib at the same concentration spiked with 0.1 mg L^{-1} of S-ibrutinib standard (**B** and **D**). (**A** and **B**) Single system (2 mM S-γ-CD), and (**C** and **D**) a dual system (2 mM S-γ-CD + 5 mM [TMA][L-Lys]). Other experimental conditions as in Fig. 3.

Table 3

Analytical characteristics of the EKC methodology developed for the determination of ibrutinib enantiomers using both 2 mM S-γ-CD and 2 mM S-γ-CD + 5 mM [TMA] [L-Lys] as chiral selectors on *D. magna* culture medium. Other experimental conditions as in Fig. 3.

	2 mM S-γ-CD		2 mM S-γ-CD + 5 mM [TMA][L-Lys]	
	S-Ibrutinib	**R-Ibrutinib**	**S-Ibrutinib**	**R-Ibrutinib**
Standard additions calibration method[a]				
D. magna culture samples				
Range	0–10 mg L^{-1}	0–10 mg L^{-1}	0–10 mg L^{-1}	0–10 mg L^{-1}
Slope ± t x S$_{slope}$	0.21 ± 0.01	0.20 ± 0.01	0.169 ± 0.009	0.176 ± 0.007
R^2	99.6%	99.6%	99.4%	99.7%
Accuracy[b]				
Recovery (%)	104 ± 5	100 ± 1	99 ± 5	98 ± 3
Precision	2 mg L^{-1}	8 mg L^{-1}	2 mg L^{-1}	8 mg L^{-1}
Instrumental repeatability[c]				
t, RSD (%)	0.3	0.5	2.4	1.4
A$_c$, RSD (%)	5.0	0.9	3.6	2.7
Method repeatability[d]				
t, RSD (%)	0.6	1.2	4.5	2.5
A$_c$, RSD (%)	5.0	3.0	5.4	3.6
Intermediate precision[e]				
t, RSD (%)	0.6	1.3	1.3	1.3
Ac, RSD (%)	4.6	3.4	3.3	4.5
LOD[f]	0.1 mg L^{-1}	0.1 mg L^{-1}	0.1 mg L^{-1}	0.1 mg L^{-1}
LOQ[f]	0.5 mg L^{-1}	0.5 mg L^{-1}	0.5 mg L^{-1}	0.5 mg L^{-1}

A$_c$: corrected peak area.

[a] Addition of five (single system) or six (dual system) known amounts of ibrutinib standard racemate solution to the culture medium of *D. magna*.

[b] Evaluated as the mean recovery obtained for ibrutinib enantiomers when six individual solutions of the ibrutinib standard racemate (n = 6) containing 4 mg L^{-1} and 16 mg L^{-1} in the culture medium of *D. magna*.

[c] Six repeated injections (n = 6) of an ibrutinib standard racemate solution at a concentration of 4 mg L^{-1} in the case of the S-enantiomer and 16 mg L^{-1} for the R-enantiomer in the culture medium of *D. magna*.

[d] Three replicates injected three times each (n = 9) on the same day of an ibrutinib standard racemate solution at a concentration of 4 mg L^{-1} in the case of the S-enantiomer and 16 mg L^{-1} for the R-enantiomer in the culture medium of *D. magna*.

[e] Three replicates injected in triplicate (n = 9) during three consecutive days of an ibrutinib standard racemate solution at a concentration of 4 mg L^{-1} in the case of the S-enantiomer and 16 mg L^{-1} for the R-enantiomer in the culture medium of *D. magna*.

[f] Calculated experimentally.

(Table 3) were compared using racemate standard solutions of ibrutinib on *D. magna* culture medium. For both methods, there were statistically significant differences between the slopes (p-values < 0.05 for a confidence interval of 95%) so it could be concluded that there were matrix interferences, and that the standard additions calibration method should be used for the enantiomeric determination of ibrutinib on *D. magna* culture medium.

To evaluate the accuracy, recovery values obtained were 104 ± 5 and 100 ± 1 for S-ibrutinib and R-ibrutinib, respectively for the single system. For the dual CD/CIL system, recovery values were 99 ± 5 and 98 ± 3 for S-ibrutinib and R-ibrutinib, respectively. In all cases, the recovery values were acceptable as they include the 100% value (see Table 3). Ibrutinib standard racemate solutions at a concentration of 4 mg L^{-1} for S-enantiomer and 16 mg L^{-1} for R-enantiomer in the culture medium were used to evaluate the precision. When the single system was used, RSD values were below 1.3% and 5.0% for migration times and corrected peak areas, respectively, while for the dual system they were lower than 4.5 and 5.4%, respectively. LOD and LOQ values were experimentally determined using the culture medium of D. magna, being 0.1 mg L^{-1} and 0.5 mg L^{-1}, respectively, for both methods and both enantiomers.

The stability of racemic and R-ibrutinib was not affected under abiotic conditions. However, under biotic conditions, the concentrations of R-ibrutinib and racemic ibrutinib were reduced in about a 20% after 24 h, being this reduction higher at 48 h (~45% for R,S-ibrutinib and ~30% for R-ibrutinib). As an example, Fig. 5 shows the electropherograms obtained for both toxics under abiotic conditions and after 24 and 48 h incubation using both EKC methods developed.

Ecotoxicity parameters obtained for 24 and 48 h of exposition time are shown in Table 4. EC$_{20}$ and EC$_{50}$ values were calculated using the real concentrations in culture media, measured by the two methods (single and dual systems). All parameters are reported with 95%

confidence interval.

As can be observed in Table 4, similar values for EC$_{20}$ and EC$_{50}$ parameters were obtained for R-ibrutinib and R,S-ibrutinib using the single and dual systems. According to the EC$_{50}$ values at 48 h and toxicity levels marked by the European Directive 93/67/EEC for aquatic ecosystems [47], R-ibrutinib and R,S ibrutinib could be categorized as toxic (1 < EC50 < 10 mg L^{-1}).

The dose-effect parameters obtained for R-ibrutinib resulted always higher than the corresponding values for R,S-ibrutinib for both exposition times (24 and 48 h). This shows that the ecotoxicity of the racemate is greater than that of the R-enantiomer. In addition, toxicological effects of R,S-ibrutinib and R-ibrutinib increased with incubation times, with increments of about 42% and 57% for EC$_{50}$ values, and of about 17% and 27% for EC$_{20}$ values, respectively, regardless the method used for the determination of real concentrations.

No ecotoxicity parameters have previously been reported in the literature for R-ibrutinib and R,S-ibrutinib. Unfortunately, no experimental ecotoxicological evidence is available for comparison. In contrast, information was found regarding toxicity of anticancer drugs on microcrustacean. Tkaczyk et al. [48] reported toxicity for four cytostatic pharmaceuticals (cytarabine, gemcitabine, 5-fluorouracil, and sunitinib), the EC$_{50}$ values for *D. magna* ranging from 200 mg L^{-1} to 15 mg L^{-1} for a 48 h of exposition time. A value of 0.48 mg L^{-1} was obtained for EC$_{50}$ for the tyrokinase inhibitor sunitinib in a chronic test of 21 days of exposition time. Parrella et al. [49] evaluated the negative effect caused by imatinib (a tyrosine kinase inhibitor) on *D. magna*, resulting a EC$_{50}$ value of 11.97 (9.37–15.45) mg L^{-1} at 48 h exposition time. The results reported for all the above-mentioned cytostatics show that these pharmaceuticals are less toxic for the aquatic life than ibrutinib although it must be taken into account that initial (not real) concentrations were employed to calculate toxicity parameters.

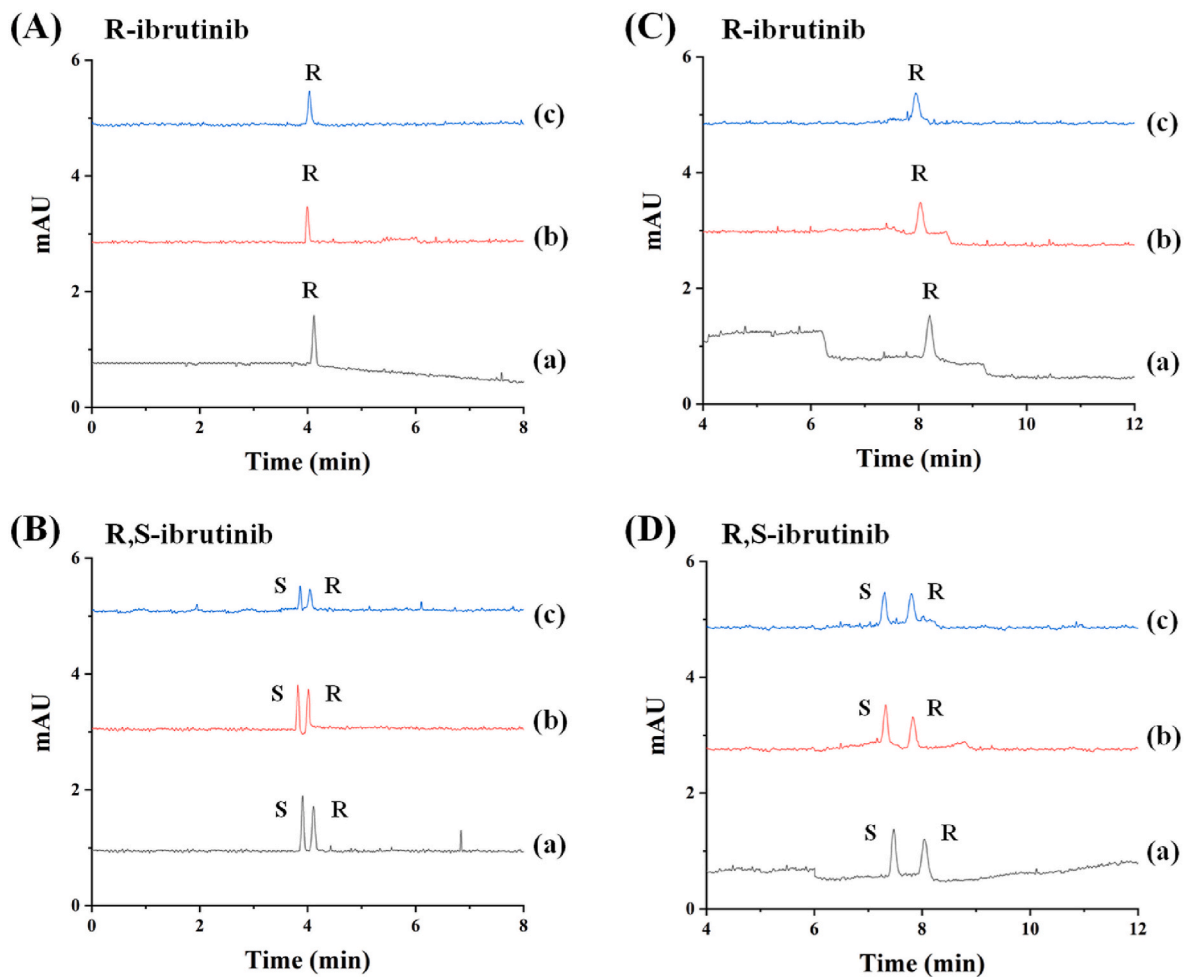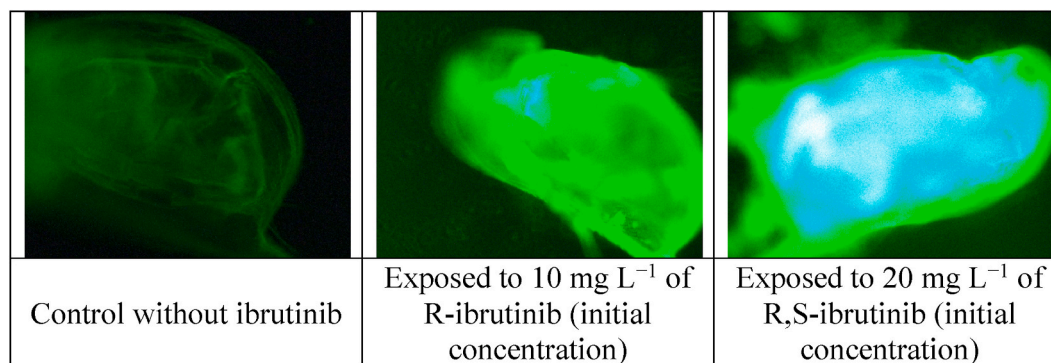Regarding ROS generation, there are previous evidence on oxidative

Fig. 5. Electropherograms corresponding to a solution of 4 mg L^{-1} R-ibrutinib, and 8 mg L^{-1} R,S-ibrutinib, under the following conditions: **(a)** 0 h under abiotic conditions, **(b)** 24 h under biotic conditions, and **(c)** 48 h under biotic conditions, using **(A, B)** 2 mM sulfated-γ-CD and **(C, D)** 2 mM sulfated-γ-CD + 5 mM [TMA] [L-Lys].

Table 4

Dose-effect parameters for R-ibrutinib and R,S-ibrutinib on *D. magna*, evaluated using real concentrations of enantiomers determined by single and dual systems.

		EC$_{20}$ (mg L^{-1})		EC$_{50}$ (mg L^{-1})	
		Single system	Dual system	Single system	Dual system
24 h	**R-Ibrutinib**	4 ± 1	3.5 ± 0.6	11 ± 1	11.6 ± 0.6
	R,S-Ibrutinib	2.1 ± 0.9	2.3 ± 0.9	7.6 ± 0.7	7 ± 1
48 h	**R-Ibrutinib**	2.5 ± 0.4	2.6 ± 0.3	4.9 ± 0.3	4.8 ± 0.2
	R,S-Ibrutinib	1.8 ± 0.8	1.9 ± 0.7	4 ± 1	4 ± 1

Control without ibrutinib	Exposed to 10 mg L^{-1} of R-ibrutinib (initial concentration)	Exposed to 20 mg L^{-1} of R,S-ibrutinib (initial concentration)

Fig. 6. Fluorescence microscopy images showing ROS generation in specimens of *D. magna* at 24 h of incubation time.

stress caused by chemicals on *D. magna* [43,50]. In the case of ibrutinib, Fig. 6 shows the oxidative stress caused by both toxics at 24 h of incubation time. This is the first evidence of the oxidative stress caused by a cytostatic on microcrustacean since experimental evidence reported are limited to human tissue cells [51,52]. Just a study on the effect of cytostatic drugs on *D. magna* was described by evaluating the activity of dismutase superoxide enzyme, which is considered the first cellular defense against oxidative stress [53]. Authors observed that the activity of this enzyme increased in the presence of these drugs, and they associated this effect to a possible increment of ROS.

4. Conclusions

Two chiral EKC methodologies enabling the enantiomeric determination of ibrutinib using a CD as chiral selector or its combination with a CIL were developed and compared. Using 2 mM S-γ-CD as chiral selector in 25 mM formate buffer at pH 3.0 at 30 °C and −30 kV gave rise to the enantioseparation of ibrutinib in 4.2 min with a resolution value of 1.5. Under these conditions, the effect of the addition of fifteen CILs to the separation medium was investigated resulting generally in an increase in both analysis time and resolution. These results can be explained considering the changes in the viscosity of the separation medium that the presence of a CIL causes as well as the interactions between the CIL and the CD, which also alter the analyte-CD interactions. Amino acids-based CILs with TMA as cationic counterpart and at a 5 mM concentration showed in general the most interesting results in terms of analysis time and resolution. The combination of 2 mM S-γ-CD with 5 mM [TMA][L-Lys] allowed the enantiomeric separation of ibrutinib in 8.1 min with a resolution of 3.3. The adequate analytical characteristics of the developed methods enabled their application to the enantiomeric analysis of a pharmaceutical formulation for hospital use marketed as pure enantiomer (R-ibrutinib). Both methods enabled to detect up to a 0.1% of the enantiomeric impurity of ibrutinib as established by the ICH guidelines. Quantitative analysis of R-ibrutinib in the pharmaceutical formulation showed a good agreement with the labeled amount while the enantiomeric impurity (S-ibrutinib) was not detected. The developed methods were also applied to the stability and ecotoxicity evaluation of R,S- and R-ibrutinib on the microcrustacean *D. magna* showing a

higher toxicity than the few cytostatics whose ecotoxicity was previously evaluated. The first evidence of oxidative stress caused by a cystostatic on microcrustaceans is presented. The two chiral EKC methods developed enabled for the first time the rapid enantiomeric separation of ibrutinib and its quantitation in pharmaceutical formulations and have demonstrated their great potential to achieve an adequate quality control of enantiopure R-ibrutinib-based pharmaceutical formulations and to evaluate the ecotoxicity of racemic and R-ibrutinib at an enantiomeric level.

CRediT authorship contribution statement

Laura García Cansino: Investigation, Formal analysis, Validation, Data curation, Visualization, Writing – original draft, Writing – review & editing. **Karina Boltes:** Methodology, Formal analysis, Validation, Resources, Supervision, Writing – original draft, Writing – review & editing, Project administration, Funding acquisition. **María Luisa Marina:** Conceptualization, Methodology, Formal analysis, Validation, Resources, Supervision, Writing – original draft, Writing – review & editing, Project administration, Funding acquisition. **María Ángeles García:** Conceptualization, Methodology, Formal analysis, Validation, Resources, Supervision, Writing – original draft, Writing – review & editing, Project administration, Funding acquisition.

Declaration of competing interest

rMaría Ángeles García reports financial support was provided by University of Alcalá. María Luisa Marina and María Ángeles García report financial support was provided by Spanish Ministry of Science and Innovation. Karina Boltes reports financial support was provided by General Council of Universities and Research of Community of Madrid.

Data availability

No data was used for the research described in the article.

Appendix A. Supplementary data

Supplementary data to this article can be found online at https://doi.org/10.1016/j.talanta.2023.124783.

References

[1] B. Chankvetadze, Application of enantioselective separation techniques to bioanalysis of chiral drugs and their metabolites, TrAC, Trends Anal. Chem. 143 (2021), 116332, https://doi.org/10.1016/j.trac.2021.116332.

[2] P. Lees, R.P. Hunter, P.T. Reeves, P.L. Toutain, Pharmacokinetics and pharmacodynamics of stereoisomeric drugs with particular reference to bioequivalence determination, J. Vet. Pharmacol. Therap. 35 (2012) 17–30, https://doi.org/10.1111/j.1365-2885.2012.01367.x.

[3] Q3B, Impurities in New Dug Products, International Conference of Harmonization, 2006.

[4] Commission Implementing Decision (EU), 1161 of 4 August 2020 Establishing a Watch List of Substances for Union-wide Monitoring in the Field of Water Policy Pursuant to Directive 2008/105/EC of the European Parliament and of the Council, 2020 (notified under document number C(2020) 5205), https://eur-lex.europa.eu/eli/dec_impl/2020/1161/oj.

[5] Y. Zhou, S. Wu, H. Zhou, H. Huang, J. Zhao, Y. Deng, H. Wang, Y. Yang, J. Yang, L. Luo, Chiral pharmaceuticals: environment sources, potential human health impacts, remediation technologies and future perspective, Environ. Int. 121 (1) (2018) 523–537, https://doi.org/10.1016/j.envint.2018.09.041.

[6] C. Mejías, M. Arenas, J. Martín, A systematic review on distribution and ecological risk assessment for chiral pharmaceuticals in environmental compartments, Rev. Environ. Contam. Toxicol. 260 (2022) 3, https://doi.org/10.1007/s44169-021-00003-5.

[7] A.C. Johnson, M.D. Jürgens, R.J. Williams, K. Kümmerer, A. Kortenkamp, J. P. Sumpter, Do cytotoxic chemotherapy drugs discharged into rivers pose a risk to the environment and human health? An overview and UK case study, J. Hydrol. 348 (1–2) (2008) 167–175, https://doi.org/10.1016/j.jhydrol.2007.09.054.

[8] M. Mišík, M. Filipic, A. Nersesyan, M. Kundi, M. Isidori, S. Knasmueller, Environmental risk assessment of widely used anticancer drugs (5-fluorouracil, cisplatin, etoposide, imatinib mesylate), Water Res. 164 (2019) 114953, https://doi.org/10.1016/j.watres.2019.114953.

[9] Directive 2008/98/EC of the European Parliament and of the Council of 19 November 2008 on Waste and Repealing Certain Directives. https://eur-lex.europa.eu/legal-content/EN/ALL/?uri=CELEX%3A32008L0098.

[10] E.O. Omotola, A.O. Oluwole, P.O. Oladoye, O.S. Olatunji, Occurrence, detection and ecotoxicity studies of selected pharmaceuticals in aqueous ecosystems- a systematic appraisal, Environ. Toxicol. Pharmacol. 91 (2022), 103831, https://doi.org/10.1016/j.etap.2022.103831.

[11] A.M. Wormington, M. De María, H.G. Kurita, J.H. Bisesi Jr., N.D. Denslow, C. J. Martyniuka, Antineoplastic agents: environmental prevalence and adverse outcomes in aquatic organisms, Environ. Toxicol. Chem. 39 (5) (2020) 967–985, https://doi.org/10.1002/etc.4687.

[12] E. Sánchez-López, M. Castro-Puyana, M.L. Marina, Capillary Electrophoresis: Chiral Separations, third ed., Encyclopedia of Analytical Science, 2019, pp. 334–345.

[13] S. Bernardo-Bermejo, E. Sánchez-López, M. Castro-Puyana, M.L. Marina, Chiral capillary Electrophoresis, TrAC, Trends Anal. Chem. 124 (2020), 115807, https://doi.org/10.1016/j.trac.2020.115807.

[14] J.M. Saz, M.L. Marina, Recent Advances on the use of cyclodextrins in the chiral analysis of drugs by Capillary Electrophoresis, J. Chromatogr., A 1467 (2016) 79–94, https://doi.org/10.1016/j.chroma.2016.08.029.

[15] I.J. Stavrou, E.A. Agathokleous, C.P. Kapnissi-Christodoulou, Chiral Selectors in CE: recent development and applications (mid-2014 to mid-2016), Electrophoresis 38 (2017) 786–819, https://doi.org/10.1002/elps.201600322.

[16] B. Chankvetadze, Contemporary theory of enantioseparations in capillary Electrophoresis, J. Chromatogr., A 1567 (2018) 2–25, https://doi.org/10.1016/j.chroma.2018.07.041.

[17] R.B. Yu, J.P. Quirino, Chiral selectors in capillary Electrophoresis: trends during 2017-2018, Molecules 24 (2019) 1135, https://doi.org/10.3390/molecules24061135.

[18] R.B. Yu, J.P. Quirino, Ionic liquids in electrokinetic Chromatography, J. Chromatogr., A 1637 (2021), 461801, https://doi.org/10.1016/j.chroma.2020.461801.

[19] L. Nie, A. Yohannes, S. Yao, Recent advances in the enantioseparation promoted by ionic liquids and their resolution mechanism, J. Chromatogr., A 1626 (2020), 461384, https://doi.org/10.1016/j.chroma.2020.461384.

[20] J.P. Hallett, T. Welton, Room-temperature ionic liquids: solvents for synthesis and catalysis 2, Chem. Rev. 111 (2011) 3508–3576, https://doi.org/10.1021/cr1003248.

[21] D.K. Bwambok, H.M. Marwani, V.E. Fernand, S.O. Fakayode, M. Lowry, I. Negulescu, R.M. Strongin, I.M. Warner, Synthesis and characterization of novel chiral ionic liquids and investigation of their enantiomeric recognition properties, Chirality 20 (2008) 151–158, https://doi.org/10.1002/chir.20517.

[22] M. Greño, M.L. Marina, M. Castro-Puyana, Enantioseparation by Capillary Electrophoresis using ionic liquids as chiral selectors, Crit. Rev. Anal. Chem. 48 (6) (2018) 429–446, https://doi.org/10.1080/10408347.2018.1439365.

[23] L. García-Cansino, M.L. Marina, M.A. García, Effect of ionic liquids and deep eutectic solvents on the enantiomeric separation of clopidogrel by Cyclodextrin-Electrokinetic Chromatography. Quantitative analysis in pharmaceutical formulations using tetrabutylammonium l-aspartic acid combined with carboxymethyl-γ-cyclodextrin, Microchem. J. 171 (2021), 106815, https://doi.org/10.1016/j.microc.2021.106815.

[24] Q. Zhang, J. Zhang, S. Xue, M. Rui, B. Gao, A. Li, J. Bai, Z. Yin, E.M. Anochie, Enhanced enantioselectivity of native α-cyclodextrins by the synergy of chiral ionic liquids in Capillary Electrophoresis, J. Separ. Sci. 41 (2018) 4525–4532, https://doi.org/10.1002/jssc.201800792.

[25] S. Salido-Fortuna, M. Greño, M. Castro-Puyana, M.L. Marina, Amino acid chiral ionic liquids combined with hydroxypropyl-β-cyclodextrin for drug enantioseparation by Capillary Electrophoresis, J. Chromatogr., A 1607 (2019), 460375, https://doi.org/10.1016/j.chroma.2019.460375.

[26] M. Greño, M. Castro-Puyana, M.L. Marina, Enantiomeric separation of homocysteine and cysteine by Electrokinetic Chromatography using mixtures of γ-cyclodextrin and carnitine-based ionic liquids, Microchem. J. 157 (2020), 105070, https://doi.org/10.1016/j.microc.2020.105070.

[27] M. Greño, M.L. Marina, M. Castro-Puyana, Use of single and dual systems of γ-cyclodextrin or γ-cyclodextrin/L-carnitine derived ionic liquid for the enantiomeric determination of cysteine by Electrokinetic Chromatography. A comparative study, Microchem. J. 160 (2021), 106596, https://doi.org/10.1016/j.microc.2021.106596.

[28] A. Christou, I.J. Stavrou, C.P. Kapnissi-Christodoulou, Combined use of β-cyclodextrin and ionic liquid as electrolyte additives in EKC for separation and determination of carob's phenolics-a study of the synergistic effect, Electrophoresis 42 (19) (2021) 1945–1955, https://doi.org/10.1002/elps.202100085.

[29] S. Salido-Fortuna, M.I. Fernández-Bachiller, M.L. Marina, M. Castro-Puyana, Synthesis and characterization of carnitine-based ionic liquids and their evaluation as additives in Cyclodextrin-Electrokinetic Chromatography for the chiral separation of thiol amino acids, J. Chromatogr., A 1670 (2022), 462955, https://doi.org/10.1016/j.chroma.2022.462955.

[30] Q. Zhang, Y. Du, J. Zhang, Z. Feng, Y. Zhang, X. Li, Tetramethylammonium-Lactobionate: a novel ionic liquid chiral selector based on saccharides in Capillary Electrophoresis, Electrophoresis 36 (2015) 1216–1223, https://doi.org/10.1002/elps.201400053.

[31] Q. Zhang, S. Ren, C. Gu, A. Li, S. Xue, Enhanced enantioselectivity of tartaric acid in Capillary Electrophoresis: from tartaric acid to tartaric acid-based ionic liquid, J. Mol. Liq. 327 (2021), 114840, https://doi.org/10.1016/j.molliq.2020.114840.

[32] Q. Zhang, S. Ren, A. Li, J. Zhang, S. Xue, X. Sun, Tartaric acid-based ionic liquid type chiral selectors: effect of cation species on their enantioseparation performance in Capillary Electrophoresis, Sep. Purif. Technol. 275 (2021), 119228, https://doi.org/10.1016/j.seppur.2021.119228.

[33] Y. Su, X. Mu, L. Qi, Development of a Capillary Electrophoresis System with Mn(II) complexes and β-cyclodextrin as the dual chiral selectors for enantioseparation of dansyl amino acids and its application in screening enzyme inhibitors, RSC Adv. 5 (2015) 28762–28768, https://doi.org/10.1039/C5RA02744F.

[34] J. Jiang, X. Mu, J. Qiao, Y. Su, L. Qi, New chiral ligand exchange Capillary Electrophoresis System with chiral amino amide ionic liquids as ligands, Talanta 175 (2017) 451–456, https://doi.org/10.1016/j.talanta.2017.07.052.

[35] S. Xue, S. Ren, L. Wang, Q. Zhang, Evaluation of tetraalkylammonium amino acid ionic liquids as chiral ligands in Ligand-Exchange Capillary Electrophoresis, J. Chromatogr., A 1611 (2020), 460579, https://doi.org/10.1016/j.chroma.2019.460579.

[36] Food and Drug Administration (FDA) Approves Imbruvica. https://www.drugs.com/newdrugs/fda-approves-imbruvica-ibrutinib-mantle-cell-lymphoma-3960.html (accessed 20 May 2022).

[37] R.R. Goppireddy, A. Maruthapillai, S. Mahapatra, M. Tamilselvi, Development and validation of HPLC method for enantioseparation of ibrutinib on immobilized chiral stationary phase, Mater. Today: Proc. 50 (2022) 384–387, https://doi.org/10.1016/j.matpr.2021.08.358.

[38] R. de Vries, M. Huang, N. Bode, P. Jejurkar, J. de Jong, J. Sukbuntherng, L. Sips, N. Weng, P. Timmerman, T. Verhaeghe, Bioanalysis of ibrutinib and its active metabolite in human plasma: selectivity issue, impact assessment and resolution, Bioanalysis 7 (20) (2015), https://doi.org/10.4155/bio.15.159.

[39] L. García-Cansino, J.M. Saz, M.A. García, M.L. Marina, Modeling the simultaneous chiral separation of a mixture of drugs by Electrokinetic Chromatography with dual systems of cyclodextrins, J. Chromatogr., A 1681 (2022), 463444, https://doi.org/10.1016/j.chroma.2022.463444.

[40] N. Casado, A. Salgado, M. Castro-Puyana, M.A. García, M.L. Marina, Enantiomeric separation of ivabradine by Cyclodextrin-Electrokinetic Chromatography, effect of amino acid chiral ionic liquids, J. Chromatogr., A 1608 (2019), 460407, https://doi.org/10.1016/j.chroma.2019.460407.

[41] OECD, *Test No. 202: Daphnia Sp. Acute Immobilisation Test*, OECD Guidelines for the Testing of Chemicals, Section 2, OECD Publishing, Paris, 2004, https://doi.org/10.1787/9789264069947-en.

[42] T.C. Chou, N. Martin, CompuSyn for Drug Combinations: PC Software and User's Guide: A Computer Program for Quantitation of Synergism and Antagonism in Drug Combinations, and the Determination of IC50 and ED50 and LD50 Values, ComboSyn, Paramus (NJ), 2005.

[43] J. Valimaña-Traverso, G. Amariei, K. Bolter, M.Á. García, M.L. Marina, Enantiomer stability and combined toxicity of duloxetine and econazole on *Daphnia magna* using real concentrations determined by Capillary Electrophoresis, Sci. Total Environ. 670 (2019) 770–778, https://doi.org/10.1016/j.scitotenv.2019.03.208.

[44] E. Galdiero, A. Falanga, A. Siciliano, V. Maselli, M. Guida, R. Carotenuto, M. Tussellino, L. Lombardi, G. Benvenuto, S. Galdiero, *Daphnia magna* and *Xenopus laevis* as in vivo models to probe toxicity and uptake of quantum dots functionalized with gH625, Int. J. Nanomed. 12 (2017) 2717–2731, https://doi.org/10.2147/IJN.S127226.

[45] N. Konduru, R. Gundla, N.K. Katari, K. Paidikondala, A.S. Reddy, V. Jagadabi, Development and validation of a stability indicating method for ibrutinib: identification and separation of degradation products, known and genotoxic impurities using RP-HPLC/PDA and QDa Mass Detectors, Anal. Chem. Lett. 10 (1) (2020) 113–136, https://doi.org/10.1080/22297928.2019.1673814.

[46] European Pharmacopoeia, fourth ed., The European Pharmacopoeia Convention Inc., 2004, pp. 3843–3849, supplement 4.6.

[47] Commission Directive 93/67/EEC of 20 July 1993 laying down the principles for assessment of risks to man and the environment of subtances notified in accordance with Council Directive 67/548/EEC (Official Journal L 227 , 08/09/1993 9-18). https://eur-lex.europa.eu/legal-content/EN/ALL/?uri=CELEX:31993L0067.

[48] A. Tkaczyk, A. Bownik, J. Dudka, K. Kowal, B. Ślaska, *Daphnia magna* model in the toxicity assessment of pharmaceuticals: a review, Sci. Total Environ. 763 (2021), 143038, https://doi.org/10.1016/j.scitotenv.2020.143038.

[49] A. Parrella, M. Lavorgna, E. Criscuolo, C. Russo, V. Fiumano, M. Isidori, Acute and chronic toxicity of six anticancer drugs on rotifers and crustaceans, Chemosphere 155 (2014) 59–66, https://doi.org/10.1016/j.chemosphere.2014.01.013.

[50] M. Greño, G. Amariei, K. Boltes, M. Castro-Puyana, M.Á. García, M.L. Marina, Ecotoxicity evaluation of tetramethrin and analysis in agrochemical formulations using Chiral Electrokinetic Chromatography, Sci. Total Environ. 800 (2021), 149496, https://doi.org/10.1016/j.scitotenv.2021.149496.

[51] S.J. Kim, H.S. Kim, Y.R. Seo, Understanding of ROS-inducing strategy in anticancer therapy, Oxid. Med. Cell. Longev. 2019 (2019) 12, https://doi.org/10.1155/2019/5381692.

[52] G. Radha, S. Raghunandhakumar, S. Balakumar, Dual therapeutic 5-fluorouracil and hesperidin loaded chitosan nanocarrier system: understanding its synergism on anti-cancer activity, J. Drug Deliv. Sci. Technol. 80 (2023) 104184, https://doi.org/10.1016/j.jddst.2023.104184.

[53] D. Mielecki, E. Grzesiuk, A. Bednarska, D. Garbicz, B. Świderska, M. Grzesiuk, Contamination of aquatic environment with anticancer reagents influences Daphnia magna-Ecotoxicogenomics approach, Ecotoxicol. Environ. Saf. 249 (2023) 114372, https://doi.org/10.1016/j.ecoenv.2022.114372.